Coordination Chemistry of 1,3-Bis(2-pyridylimino)- and 1,3-Bis-(2-thiazolylimino)isoindole Copper Complexes: Investigation of Their Catalytic Behavior in Oxidation Reactions

Markus B. Meder[a] and Lutz H. Gade*[a,b]

Keywords: Copper / Allylic peroxylation / Coordination polymers / Radical reactions / Oxidation

The copper complexes [Cu(4-MeBPI)(OAc)] (**4**), [Cu(4-Me-10-*t*BuBPI)(OAc)] (**5**) and [Cu(BTI)(OAc)] (**6**) [BPI = 1,3-bis(2-pyridylimino)isoindole, BTI = 1,3-bis(2-thiazolylimino)isoindole] were prepared by reaction of the protio ligands with copper(II) acetate. Compounds **4** and **6** were characterized by X-ray diffraction, establishing distorted square-planar coordination geometries of the copper ions. Two monoclinic modifications of **6** (**6a** and **6b**) were found, both crystallizing in the space group $P2_1/c$, but possessing different cell parameters. In contrast to **6a**, which is monomeric in the crystal, the second monoclinic modification **6b** has a more complicated crystal structure, which is composed of both monomeric complex units such as those found in **6a** and infinite chains of coordination polymers. The copper atoms in the polymeric chains of **6b** display fivefold coordination and a ligand polyhedron that is an intermediate form between a trigonal-bipyramidal and a square-pyramidal geometry. The allylic peroxylation of cyclohexene with *t*BuOOH (70% aqueous solution) catalyzed by **4** and **6** (0.17 mol %) gave *tert*-butylperoxy-3-cyclohexene with selectivities of 86% and 80% (based on cyclohexene) and turnover frequencies of 63 h^{-1} and 18 h^{-1}, respectively. The peroxylation reaction is thought to proceed according to a Haber–Weiss radical chain mechanism.

Introduction

The direct oxidation of C−H bonds is an important chemical transformation in organic synthesis. A preparatively useful example of such a conversion of hydrocarbons is the copper-catalyzed Kharasch−Sosnovsky reaction, i.e. the allylic acyloxylation of olefins [Equation (1)].[1] In the presence of chiral oxazoline-based ligands it has been possible to render this reaction enantioselective,[2] although a truly efficient asymmetric catalyst has not as yet been found. A much less studied variant of this oxidation is the allylic peroxylation, which is also catalyzed by Cu salts [Equation (2)]. The synthesis of dialkyl peroxides by the oxidation of cycloolefins with *tert*-butyl hydroperoxide, first reported by Kharasch,[3] has recently attracted renewed attention due to the high diastereoselectivity of the subsequent epoxidation or dihydroxylation of the C=C bond.[4] This gives rise to highly functionalized cyclohexane derivatives.

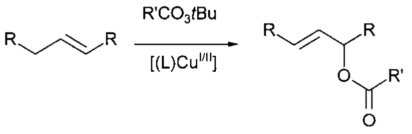

(1)

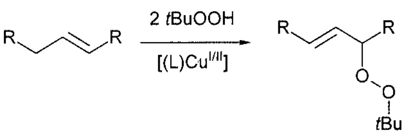

(2)

In the standard reaction protocols for allylic peroxylations, a Cu^I or Cu^{II} salt and, occasionally, an N-donor ligand are added to the reaction mixture which assemble to give the active catalyst, the nature of which is generally not unambiguously established.

In this paper we report the synthesis and structural characterization of several Cu^{II} complexes containing 1,3-bis(2-pyridylimino)isoindole (BPI) and 1,3-bis(2-thiazolylimino)isoindole (BTI) ligands, and their use as selective catalysts in the allylic peroxylation of cyclohexene. First reported in the 1950s,[5] such tridentate ligands have more recently been employed by Siegl and co-workers in the tran-

---

[a] Laboratoire de Chimie Organométallique et de Catalyse (CNRS UMR 7513), Institut Le Bel, Université Louis Pasteur, 4, rue Blaise Pascal, 67000 Strasbourg, France
[b] Anorganisch-Chemisches Institut, Universität Heidelberg, Im Neuenheimer Feld 270, 69120 Heidelberg, Germany
E-mail: lutz.gade@uni-hd.de

sition-metal (mainly cobalt) catalyzed oxidation of saturated hydrocarbons.[6,7] In a systematic study of the cobalt-catalyzed oxidation of cyclohexane and cyclohexene, Mimoun et al. employed *tert*-butyl hydroperoxide as the oxidizing reagent;[8] furthermore, the photoactivation of this kind of BPI-metal peroxo complex for the oxidation of hydrocarbons has also been reported.[9] Given the facile accessibility of well-defined BPI and BTI transition metal complexes and the previous results on copper-catalyzed allylic peroxylations, copper complexes of isoindole-derived tridentate ligands appear to be promising candidates for this type of transformations.

Results and Discussion

Synthesis of the Bis(2-pyridylimino)isoindole (BPI)- and Bis(2-thiazolylimino)isoindole (BTI)-Copper Complexes

For the synthesis of the bis(2-pyridylimino)isoindole and bis(2-thiazolylimino)isoindole ligand precursors, the method previously reported by Siegl was employed.[6,7,10] The phthalodinitrile starting materials were treated with an excess of the corresponding 2-aminopyridines or 2-aminothiazole in the presence of a catalytic amount of $CaCl_2$ (Scheme 1). The use of 1-hexanol as solvent instead of 1-butanol, as is reported in the literature for this type of conversion, gave significantly improved yields of the ligand precursors 4-MeBPI (**1**), 4-Me-10-*t*BuBPI (**2**) and BTI (**3**).

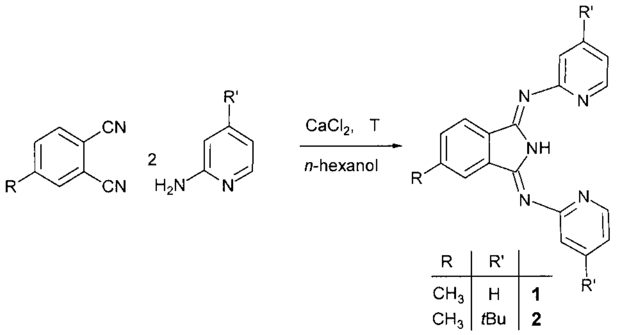

Scheme 1. Synthesis of the BPI ligands **1** and **2**

The BPI- and BTI-copper complexes [(4-MeBPI)-Cu(OAc)] (**4**), [(4-Me-10-*t*BuBPI)Cu(OAc)] (**5**), and [(BTI)-Cu(OAc)] (**6**) were prepared as previously published for similar complexes (Scheme 2 and Scheme 3);[11,12] compound **6** is the first BTI copper complex to be reported. To avoid the formation of the symmetric complexes $[Cu(BPI)_2]$ or $[Cu(BTI)_2]$, the exact metal−ligand stoichiometry was chosen, and the reaction temperature kept below 300 K. The formulation and the identity of **4**−**6** were confirmed by IR spectroscopy and elemental analysis.

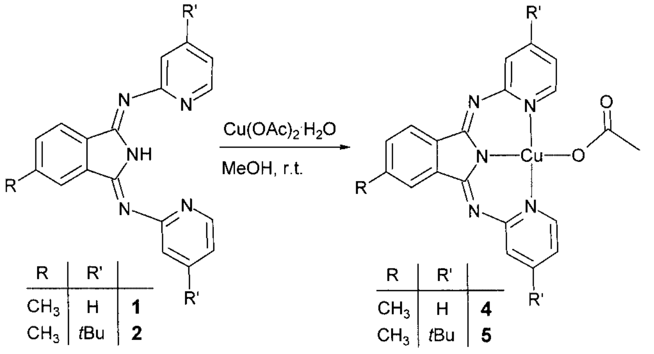

Scheme 2. Synthesis of the (acetato)(BPI)copper complexes **4** and **5**

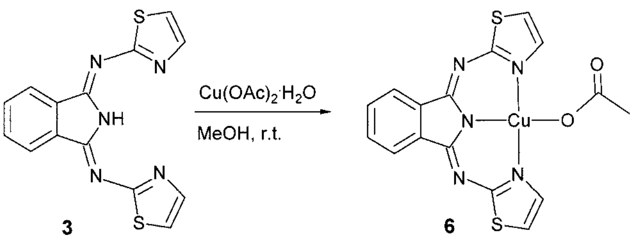

Scheme 3. Synthesis of the (acetato)(BTI)copper complex **6**

Structural Characterization of 4, 6a and 6b

Whereas a considerable number of X-ray diffraction studies have been carried out for transition-metal complexes of BPI, there are only a few previously determined structures for copper complexes. Gagné reported the dimeric structure of a (carbonato)(BPI)copper complex and the molecular structure of a μ-oxo-copper pentamer,[11] while Bereman, in a study aimed at modeling the coordination sphere of the Cu^{II} site in galactose oxidase, reported the crystal structure analysis of a pentacoordinate (acetato)(BPI)-copper complex.[13]

X-ray diffraction studies of both BPI copper compounds **4** and **5** were carried out. However, severe disorder of the *tert*-butyl groups in **5**, as well as disordered solvent in the unit cell, precluded a complete structure analysis of the latter (although the gross structural features displayed in Scheme 2 were confirmed). A single-crystal X-ray structure analysis of complex **4** established the structural details of this class of compounds. Its molecular structure is displayed in Figure 1, along with the principal bond lengths and bond angles.

As is apparent from Figure 1, the molecular structure of **4** is distorted from an ideal square-planar geometry. For instance, the N(1)−Cu−N(5) angle was found to be 158.8(1)°, which is significantly more acute than the corresponding bond angle found by Bereman et al. in the pentacoordinate complex $[(10\text{-MeBPI})Cu(OAc)(H_2O)]$ (169.4°).[13] The acetato ligand is monodentate and the Cu−O(1) distance of 1.956(2) Å is in the expected range.[14] The carboxyl group is arranged orthogonally to the metal complex plane due to steric repulsion with the pyridyl rings. This leads to an axial disposition of the O(2) atom of the carboxyl unit relative to the copper atom. However, the

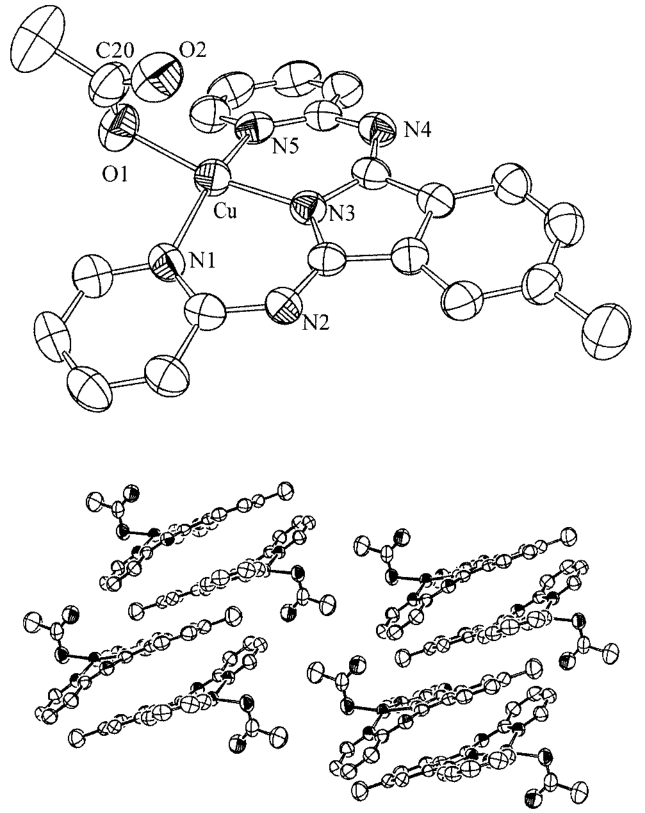

Figure 1. Molecular structure of complex **4** (top); selected bond lengths (Å) and angles (°): Cu−N(1) 2.023(3), Cu−N(3) 1.884(3), Cu−N(5) 2.014(3), Cu−O(2) 2.601(3), Cu−O(1) 1.956(2), C(20)−O(1) 1.249(5), C(20)−O(2) 1.245(5), N(1)−Cu−N(3) 90.6(1), N1−Cu−N5 158.2(1), N(1)−Cu−O(1) 93.3(1), N(3)−Cu−N(5) 89.3 (1), N(3)−Cu−O(1) 166.1(1), N(5)−Cu−O(1) 91.9(1), O(1)−C(20)−O(2) 122.9(4); view of the molecular packing of **4** in the unit cell (bottom)

Cu−O(2) distance of 2.601 Å does not support a significant bonding interaction and should be compared with the Cu−O bond length of 2.466 Å for the weakly axially coordinated water molecule in Bereman's complex.[13] A view of the packing of complex **4** in the unit cell clearly indicates that there are no bridging interactions of the acetato groups between the molecular units that stack in a head-to-tail fashion (Figure 1, bottom).

Since there is no previous report of a fully structurally characterized BTI complex, attempts were made to crystallize compound **6** in order to carry out an X-ray diffraction study. Two monoclinic crystalline modifications, the habits of which differed only marginally and which possessed identical analytical properties, were obtained in varying ratios on slow diffusion of *n*-hexane into a toluene solution of **6**. Mechanical separation of one type of crystal habit and subsequent recrystallization again gave both crystalline forms. Single-crystal X-ray structure analysis of both crystalline modifications **6a** and **6b** were carried out in order to establish the details of the molecular structure of **6** and its arrangement in both solid forms. The molecular structure of **6a** and its molecular packing pattern is displayed in Figure 2, while the principal bond lengths and bond angles are listed in Table 1.

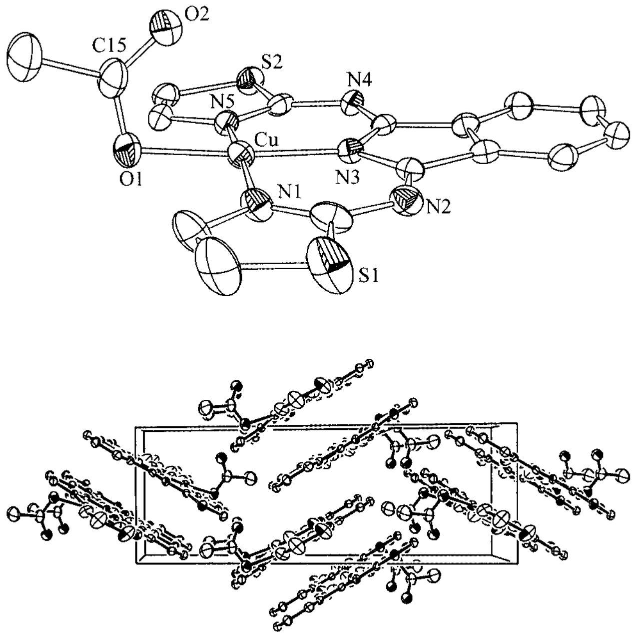

Figure 2. Molecular structure of **6a** (top); selected bond lengths and angles are given in Table 1; view of the molecular packing of **6a** in the unit cell (bottom)

Table 1. Comparison of selected bond lengths (Å) and angles (°) of **6a** and **6b**

	6a	**6b**
Cu−N1	1.991(3)	1.94(1)
Cu−N3	1.931(3)	1.98(1)
Cu−N5	1.989(3)	1.95(1)
Cu−O1	1.948(3)	2.08(1)
Cu−O2	2.595	2.54
Cu−O2′	−	2.23(1)
N1−Cu−N3	89.7(1)	89.1(5)
N1−Cu−N5	172.7(1)	173.0(5)
N3−Cu−O1	175.3(1)	154.2(5)
N3−Cu−O2	−	120.6(5)
O1−Cu−O2′	−	85.2
Cu−O1−C15	104.8(2)	101(1)
O1−C15−O2	122.8(4)	123(1)

The replacement of the pyridyl units by thiazolyl groups leads to a different orientation of the neutral N-donor functions and leaves a more open space for the acetate ligand than in **4**. These two factors lead to a complex geometry, which deviates less from the idealized planar structure than that found for **4**. The angles N(1)−Cu−N(5) and N(3)−Cu−O(1) are 172.7(1) and 175.3(1)°, respectively. Whereas the metal−N distance of the formally anionic donor atom is 0.05 Å greater than in **4** [**6a**: 1.931(3), **4**: 1.884(3) Å], the copper−thiazolyl-N bond lengths are about 0.03 Å shorter than the corresponding bond lengths in the BPI complex. The view of the molecular packing in **6a**, which is displayed in Figure 2, indicates a molecular head−tail stacking with interlayer distances of about 3.7

Å. There is no indication of bonding interactions through bridging acetato ligands in this structure.

In contrast to **6a**, the second monoclinic modification **6b** has a more complicated crystal structure composed of both monomeric complex units such as those found in **6a** and infinite chains of coordination polymers. A segment of such a chain structure is displayed in Figure 3, while the parameters of the complex within the polymeric structure are listed in Table 1 (those of the monomers are essentially identical to **6a**).

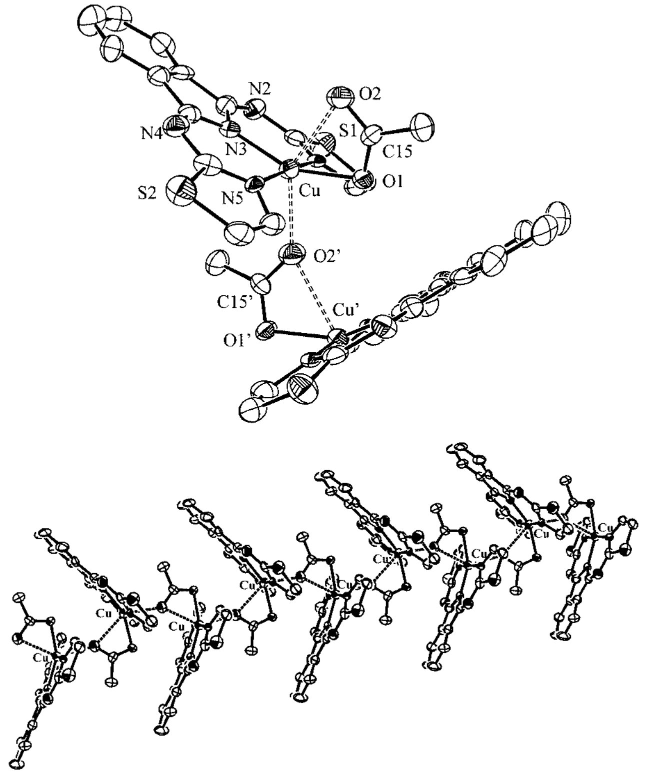

Figure 3. A segment of the chain structure in **6b** (top); selected bond lengths and angles are given in Table 1; polymeric chain structure of the (acetato)(BTI)copper complex in **6b** (bottom)

In contrast to the almost ideally planar four-coordinate structure of **6a**, the copper atoms in the polymeric chains of **6b** display fivefold coordination and a ligand polyhedron which is an intermediate form between a trigonal-bipyramidal and a square-pyramidal geometry. While the arrangement of the three heterocycles of the BTI ligand remains almost planar [N(1)−Cu−N(5), 173.0(5)°], the acetato ligand is tilted out of this plane [N(3)−Cu−O(1), 154.2(5)°], therefore making space for the coordination of the second acetato oxygen atom of a neighboring (acetato)(BTI)copper coordination unit. Significantly, the Cu−O(1) bond length of 2.08(1) Å is longer than in the square-planar monomer, and the Cu−O(2′) distance of 2.23(1) Å is indicative of substantial intermolecular bonding, leading to the polymeric complex. Similar Cu−O bond lengths were reported for two BPI copper complexes: a dimeric carbonato- and an oligomeric hydroxo-bridged complex.[12]

It should be pointed out that upon redissolution of either of the two crystalline modifications of compound **6** and subsequent recrystallization of the material, crystals of both monoclinic forms reprecipitated. The sole species in solution is therefore thought to be the monomer, as observed in **6a**. Exclusive formation of either **6a** or **6b** was not achieved by variation of either the solvent system or the temperature of crystallization.

Allylic Peroxylation of Cyclohexane Catalyzed by Complexes 4−6

In order to assess the catalytic activity of the copper complexes in the allylic peroxylation of alkenes, the Cu^{II}-catalyzed reaction of *t*BuOOH with cyclohexene was studied. In contrast to a previous study on the analogous Co-catalyzed reaction by Mimoun et al., who employed the oxidant in very high concentrations (96%),[8] we chose the commercial aqueous solution of 70% *t*BuOOH. Remarkably, all three complexes gave the dialkyl peroxide, *tert*-butylperoxy-3-cyclohexene, very selectively (Scheme 4). Conversions to this major product (based on cyclohexene) were in the range of 80−90%.

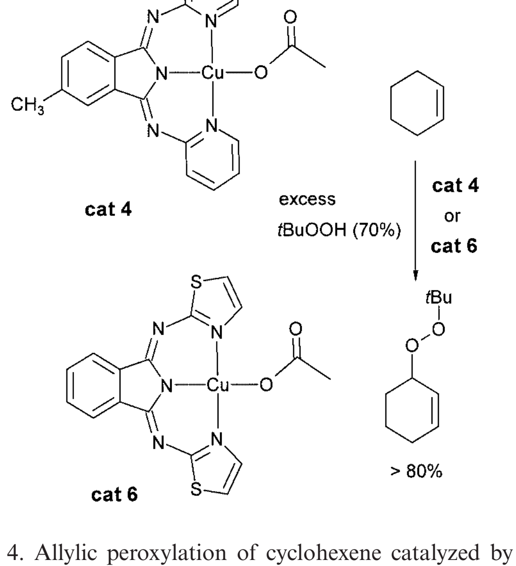

Scheme 4. Allylic peroxylation of cyclohexene catalyzed by complexes **4** and **6** giving the dialkyl peroxide in over 80% yield

The principal difference between the three catalysts was the activity observed: the two BPI derivatives display the same catalytic activity and are significantly more active than the BTI complex as is shown in Figure 4 for catalysts **4** and **6**. Both reactions were carried out with a catalyst loading of 0.17 mol %. Considering the nearly linear part of the conversion curves between 10% and 75%, the turnover frequencies amount to 63 h^{-1} for **4** and 18 h^{-1} for the BTI complex **6**. The maximum conversions of 86% observed for complex **4** and 80% for complex **6** correspond to turnover numbers of 505 and 470, respectively. The reaction product *tert*-butylperoxy-3-cyclohexene was isolated by distillation and fully characterized. In order to exclude the possibility that a simple copper salt acts as a catalytic species after initial degradation of the ligands, analogous catalytic runs using the identical reaction parameters were carried out with copper acetate. Very slow oxidation of cyclohexene was observed with low chemoselectivity; the conversion of the starting material was variable, but in all cases well below 10% after 1500 minutes (the time frame of the experiments represented in Figure 4). Thus, for the results presented in this work, the background activity of nonligated copper salts is insignificant.

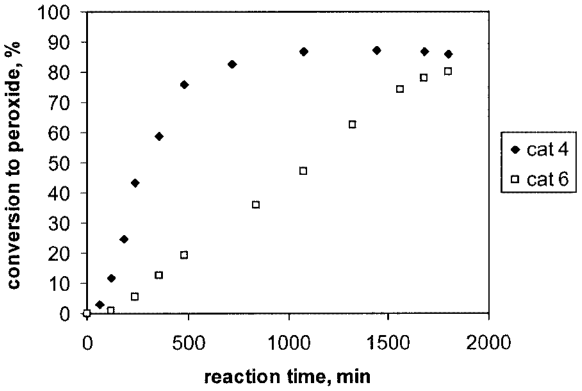

Figure 4. Peroxidation of cyclohexene with the catalysts **4** and **6**

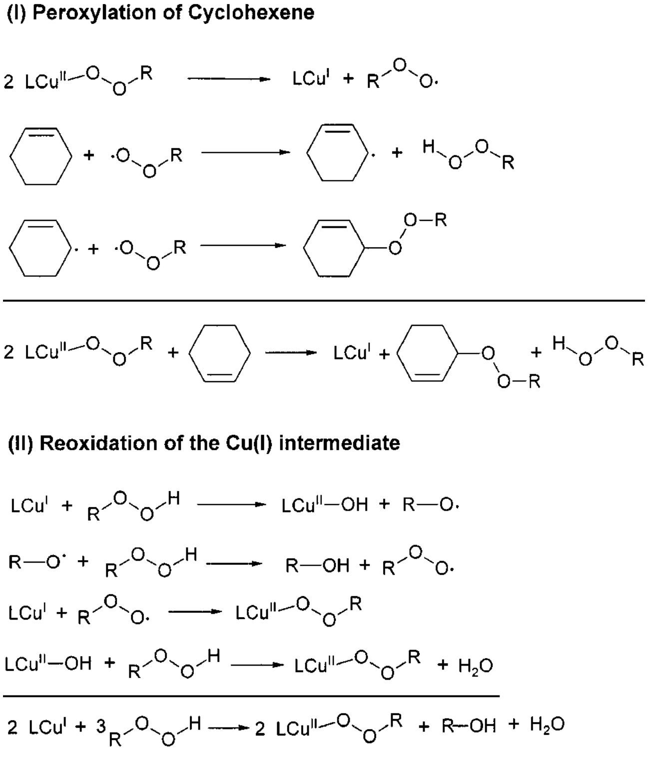

Scheme 5. Postulated Haber−Weiss mechanism for the Cu-catalyzed peroxylation: generation of the alkylperoxycopper(II) complexes as the active species and their degradation to the Cu^{I} species with concomitant transfer of the peroxyl group to the allylic position of cyclohexene

The catalytic reaction most probably proceeds according to a Haber−Weiss chain mechanism, as has been suggested previously, and which depicted in Scheme 5.[15] The active species is the copper(II) *tert*-butyl peroxide complex which thermally decomposes to the Cu^{I} complex and a peroxyl radical. This radical intermediate abstracts a hydrogen atom from the allylic position of cyclohexene, and the cyclohexenyl radical then recombines with a second peroxyl radical generated in the same way. The Cu^{I} product is then re-oxidized by the alkyl hydroperoxide in several steps generating *tert*-butanol and water as reduced products.

When the reaction product *tert*-butylperoxy-3-cyclohexene was exposed to the copper complexes over a longer period of time (> 20 h for **4** and **5** and > 35 h for **6**), slow conversion of the dialkyl peroxide to cyclohexenone and *tert*-butanol was observed (Scheme 6). This slow secondary reaction limits the yields of the dialkyl peroxide which can be isolated from the copper-catalyzed peroxylation described in this work. It was also observed by the addition of the Cu complexes to pure, isolated dialkyl peroxide.

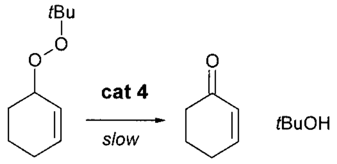

Scheme 6. Copper-catalyzed slow conversion of *tert*-butylperoxy-3-cyclohexene to cyclohexenone and *tert*-butanol

Conclusion

In this work we have presented a detailed study of the coordination chemistry of three BPI and BTI copper complexes and their activity as catalysts for the allylic peroxylation of cyclohexene as substrate of reference. Using the hydroperoxide oxidant as an aqueous solution with a concentration of 70% gave the *tert*-butyl cyclohexenyl peroxide with high selectivity. Other previously described reaction products such as 3-cyclohexenol, 3,3′-dicyclohexenyl were not observed, even in traces, while exposure of the dialkyl peroxide to the copper catalysts for an extended period of time led to a very slow degradation to cyclohexenone as a secondary product. The high selectivity of the peroxylation on use of the BPI copper compounds and the relatively high turnover numbers obtained render these systems competitive catalysts for peroxylation reactions. We are currently studying the regioselectivity of the peroxide formation for nonsymmetrical olefins in order to assess the general applicability of this method.

Experimental Section

All manipulations were performed under a nitrogen atmosphere in standard (Schlenk) glassware. Solvents were dried according to standard procedures and saturated with nitrogen. The deuterated solvents used for NMR spectroscopic measurements were degassed by three successive "freeze-pump-thaw" cycles and dried using standard techniques.

The ^1H and ^{13}C NMR spectra were recorded using an AMX 400 FT NMR spectrometer and infrared spectra on a Perkin−Elmer 1600 FT-IR spectrometer. Elemental analyses were carried out in the microanalytical laboratories of the chemistry departments at Würzburg (Germany) and Strasbourg (France). The compounds 2-amino-4-*tert*-butylpyridine[16] and 4-methylphthalonitrile[17] were prepared according to published methods. All other chemicals used as starting materials were obtained commercially and used without further purification.

Preparation of the Ligands: The synthesis of the ligand precursors was carried out by a modified protocol based on the method which was originally published by Siegl.[7,10] This modified reaction protocol will be exemplified for the synthesis of the novel derivative 4-Me-10-*t*BuBPI (**2**).

4-Me-10-*t*BuBPI (2): A suspension of 4-methylphthalonitrile (1.50 g, 10.6 mmol), 2-amino-4-*tert*-butylpyridine (3.96 g, 26.1 mmol) and $CaCl_2$ (0.16 g, 1.36 mmol) in 1-hexanol (50 cm^3) was refluxed for 18 h. After cooling to room temperature, the yellow compound which precipitated was filtered, washed with water (500 cm^3) and dried in vacuo. Yield: 2.53 g (56%). M.p. 204 °C. ^1H NMR (400.16 MHz, C_6D_6, 295 K): $\delta = 1.1, 1.2$ ($2 \times$ s, 2×9 H, 10-*t*Bu), 2.05 (s, 3 H, 4-CH_3), 6.84 (m, 2 H, 11-H), 6.94 (br. d, $^3J_{H,H} = 7.9$ Hz, 1 H, 5-H), 7.72 (m, 2 H, 9-H), 8.02 (br. s, 1 H, 3-H), 8.12 (d, $^3J_{H,H} = 7.9$ Hz, 1 H, 6-H), 8.60 (d, $^3J_{H,H} = 5.3$ Hz, 2 H, 12-H), 11.91 (br. s, 1 H, N−H). $\{^1H\}^{13}C$ NMR (100.6 MHz, C_6D_6, 295 K): $\delta = 21.6$ (4-CH_3), 30.4 [10-C(CH_3)$_3$], 34.5 [10-C(CH_3)$_3$], 117.7 (C-11), 121.1 (C-9), 122.9 (C-5), 123.6 (C-6), 132.8 (C-3), 137.2 (C-1, C-2), 141.9 (C-4), 148.1 (C-12), 154.1 (C-7), 161.8 (C-8, C-10) ppm. IR (KBr): $\tilde{\nu} = 3237$ (m, br), 2962 (m), 2867 (w), 1633 (m), 1590 (s), 1534 (w), 1477 (w), 1401 (w), 1365 (w), 1354 (w), 1310 (vw), 1285 (w), 1265 (w), 1219 (w), 1201 (vw), 1180 (vw), 1108 (vw), 1037 (vw), 928 (m), 890 (m), 826 (m), 716 (m) cm^{-1}. $C_{27}H_{31}N_5$ (425.57 g mol^{-1}): calcd. C 76.2, H 7.3, N 16.5; found C 76.5, H 7.4, N 16.3.

Preparation of the Copper Complexes

[Cu(4-MeBPI)(OAc)] (4): A suspension of **1** (87.0 mg, 0.28 mmol) was added to a stirred suspension of $Cu(OAc)_2{\cdot}H_2O$ (0.11 g, 0.56 mmol) in 10 mL of methanol at room temperature. After stirring for 16 h at room temperature, the reaction mixture was filtered and the resulting deep brown solution was concentrated in vacuo. The crude product was suspended in toluene and filtered with Celite. Evaporation of the solvent afforded a green-brown solid, which was recrystallized from toluene/*n*-hexane. Yield: 87.0 mg (71%). Green-brown crystals suitable for X-ray diffraction were grown by the slow diffusion of *n*-hexane into a saturated solution of **4** in toluene at room temperature. M.p. 116 °C. IR (KBr): $\tilde{\nu} = 2925$ (w), 1628 (m), 1597 (m), 1573 (s), 1531 (m), 1467 (m), 1460 (m), 1431 (m), 1398 (vw), 1365 (w), 1280 (w), 1184 (w), 1135 (m), 1077 (w), 1012 (w), 786 (w), 755 (w) cm^{-1}. $C_{21}H_{17}CuN_5O_2$ (434.95 g mol^{-1}): calcd. C 58.0, H 3.5, N 16.1; found C 58.1, H 3.5, N 15.9%.

[Cu(4-Me-10-*t*BuBPI)(OAc)] (5): A suspension of **2** (80.0 mg, 0.19 mmol) was added to a stirred suspension of $Cu(OAc)_2{\cdot}H_2O$ (75.0 mg, 0.38 mmol) in 10 mL of methanol at room temperature. After stirring for 16 h at room temperature, the reaction mixture was filtered and the resulting deep brown solution was concentrated in vacuo. The crude product was suspended in toluene and filtered with Celite. Evaporation of the solvent afforded a green-brown solid, which was recrystallized from toluene/*n*-hexane. Yield: 82.0 mg (79%). M.p. 124 °C. IR (KBr): $\tilde{\nu} = 2965$ (w), 1671 (m), 1573 (s), 1507 (m), 1478 (m), 1403 (m), 1360 (m), 1326 (w), 1248 (w), 1182 (m), 1143 (m), 1112 (m), 1082 (w), 946 (w), 918 (w), 885 (w), 828 (w), 729 (w) cm^{-1}. $C_{29}H_{33}CuN_5O_2$ (547.15 g mol^{-1}): calcd. C 63.7, H 6.1, N 12.8; found C 63.9, H 6.2, N 12.4%.

[Cu(BTI)(OAc)] (6a) and [Cu(BTI)(OAc)]$_\infty$ (6b): A suspension of BTI (**3**) (0.12 g, 0.38 mmol) in methanol was added to a suspension of $Cu(OAc)_2{\cdot}H_2O$ (0.15 g, 0.76 mmol) in methanol (10 mL). After stirring for 12 h at room temperature, the reaction mixture was dried in vacuo and the residue was redissolved in toluene. After filtration with Celite, the solution was concentrated and the crude product was recrystallized from toluene/*n*-hexane. Orange (**6a**) and yellow (**6b**) crystals suitable for X-ray diffraction were grown by slow diffusion of *n*-hexane into a saturated solution of **6** in toluene at room temperature. Yield: 0.13 g (81%). M.p. 121 °C. IR (KBr): $\tilde{\nu} = 3107$ (w), 2965 (vw), 1583 (m), 1542 (s), 1494 (m), 1469 (w), 1383 (m), 1308 (w), 1298 (w), 1240 (m), 1190 (m), 1102 (s), 1071 (m), 916 (vw), 877 (m), 813 (vw), 715 (m), 682 (vw) cm^{-1}. $C_{16}H_{11}CuN_5O_2S_2$ (432.97 g mol^{-1}): calcd. C 44.4%; H 2.6%; N 16.2%; found C 44.7%; H 2.7%; N 15.9%.

Catalytic Peroxylation of Cyclohexene: The catalytic peroxylations were carried out in neat cyclohexene with catalyst concentrations of 0.17 mol % and a twofold excess of *tert*-butyl hydroperoxide. Samples of ca. 10 µL were taken at the intervals indicated in Figure 4 and dissolved in 2 mL of toluene. The solution was then injected into a Shimadzu GC-17A/GCMS-QP5050A instrument. The measured ratio of the substrate and products was calibrated by comparative measurements with known ratios of pure substances. The conversion (%) generally refers to the generation of *tert*-butyl cyclohex-2-en-1-yl peroxide based on the substrate cyclohexene. The data displayed are average values of two runs.

The reaction product *tert*-butyl cyclohex-2-en-1-yl peroxide was isolated after filtration of the product mixture through a pad of Celite and removal of the solvent in vacuo. The crude product was subjected to a Kugelrohr distillation at 1 mbar (b.p. ca. 60 °C). ^1H NMR (400.16 MHz, $CDCl_3$, 295 K): $\delta = 1.25$ (s, 9 H), 1.56 (m, 1 H), 1.73 (m, 2 H), 1.94 (m, 2 H), 2.06 (m, 12 H), 4.40 (m, 1 H), 5.74 (m, 1 H), 5.95 (m, 1 H). $\{^1H\}^{13}C$ NMR (100.6 MHz, $CDCl_3$, 295 K): $\delta = 18.8, 25.7, 26.8, 27.3, 76.7, 80.0, 124.5, 133.7$ ppm. MS (EI): 170.1 [M^+].

X-ray Diffraction Study of 4, 6a and 6b: The crystal data were collected on a Nonius−Kappa CCD diffractometer at −100 °C and transferred to a DEC Alpha workstation; for all subsequent calculations the Nonius OpenMoleN package was used.[18] The structures were solved by direct methods, and absorption corrections were part of the scaling procedure of the data reductions. After refinement of the heavy atoms, difference Fourier maps revealed the maxima of residual electron density close to the positions expected for the hydrogen atoms; they were introduced as fixed contributors in the structure factor calculations with fixed coordinates (C−H: 0.95 Å) and isotropic temperature factors [$B(H) = 1.3\ B_{eqv}(C)$ Å^2], but not refined. Full least-square refinements on F^2. A final difference map revealed no significant maxima of electron density. The scattering factor coefficients and the anomalous dispersion coefficients were taken from the literature.[19] Crystal data and experimental details for the crystals of **4**, **6a** and **6b** are given in Table 2.

CCDC-228180 to -228182 contains the supplementary crystallographic data for this paper. These data can be obtained free of charge at www.ccdc.cam.ac.uk/conts/retrieving.html [or from the

Table 2. X-ray data collection and processing parameters for **4**, **6a** and **6b**

	4	**6a**	**6b**
Empirical formula	$2(C_{21}H_{17}CuN_5O_2)C_7H_8$	$C_{16}H_{11}CuN_5O_2S_2$	$C_{16}H_{11}CuN_5O_2S_2$
M	962.03	432.97	432.97
Temp. [°C]	21(1)	−100(1)	−100(1)
Wavelength. [Å]	0.71073	0.71073	0.71073
Space group	$P\bar{1}$	$P2_1/c$	$P2_1/c$
a [Å]	8.3873(5)	10.7706(6)	5.4021(6)
b [Å]	9.2129(5)	7.6486(4)	8.4923(2)
c [Å]	14.8935(9)	21.383(1)	25.679(1)
α [°]	92.069(5)	−	−
β [°]	91.730(5)	101.577(5)	91.743(5)
γ [°]	103.686(5)	−	−
V [Å^3]	1116.5(2)	1725.7(2)	3357.2(3)
Z	1	4	8
$D_{calcd.}$ [g cm^{-3}]	1.43	1.67	1.71
Abs. coeff./[mm^{-1}]	1.010	1.529	1.572
R indices	$R_1 = 0.046$	$R_1 = 0.035$	$R_1 = 0.092$
	$R_w = 0.065$	$R_w = 0.041$	$R_w = 0.141$

Cambridge Crystallographic Data Centre, 12 Union Road, Cambridge CB2 1EZ, UK; Fax: (internat.) +44-1223-336-033; E-mail: deposit@ccdc.cam.ac.uk].

Acknowledgments

We thank the Deutsche Forschungsgemeinschaft, the CNRS (France) and the Institut Universitaire de France for financial support of this work. We are grateful to Dr. André De Cian and N. Gruber for the X-ray diffraction studies.

---

[1] [1a] M. S. Kharasch, G. Sosnovsky, *J. Am. Chem. Soc.* **1958**, *80*, 756−757. [1b] M. S. Kharasch, G. Sosnovsky, *J. Am. Chem. Soc.* **1959**, *81*, 5819−5824.

[2] Selected early reports of asymmetric Kharasch−Sosnovsky reactions: [2a] A. S. Gokhale, A. B. E. Minidis, A. Pfaltz, *Tetrahedron Lett.* **1995**, *36*, 1831−1834. [2b] M. B. Andrus, A. B. Argade, X. Chen, M. G. Pamment, *Tetrahedron Lett.* **1995**, *36*, 2945−2948. [2c] K. Kawasaki, S. Tsumura, T. Katsuki, *Synlett* **1995**, 1245−1246. [2d] A. Levina, J. Muzart, *Tetrahedron: Asymmetry* **1995**, *6*, 147−156. Recent reviews: [2e] M. B. Andrus, J. C. Lashley, *Tetrahedron* **2002**, *58*, 845−866. [2f] J. Eames, M. Watkinson, *Angew. Chem. Int. Ed.* **2001**, *40*, 3567−3571.

[3] [3a] M. S. Kharasch, P. Pauson, W. Nudenberg, *J. Org. Chem.* **1953**, *18*, 322−327. [3b] W. Treibs, G. Pellmann, *Chem. Ber.* **1954**, *87*, 1201−1205. [3c] M. S. Kharasch, A. Fono, *J. Org. Chem.* **1958**, *23*, 324−325. [3d] M. S. Kharasch, A. Fono, *J. Org. Chem.* **1959**, *24*, 72−78.

[4] [4a] M. Schulz, R. Kluge, F. G. Gelalcha, *Tetrahedron: Asymmetry* **1998**, *9*, 4341−4360. [4b] M. Schulz, R. Kluge, S. Liebsch, J. Lessig, M. Halik, F. G. Gelalcha, *Tetrahedron* **1996**, *52*, 13151−13166.

[5] J. A. Elvidge, R. P. Linsted, *J. Chem. Soc.* **1952**, 5008−5012.

[6] [6a] W. O. Siegl, *J. Org. Chem.* **1977**, *42*, 1872−1878. [6b] W. O. Siegl, *Inorg. Nucl. Chem. Letters* **1974**, *10*, 825−829.

[7] R. R. Gagné, W. A. Marritt, D. N. Marks, W. O. Siegl, *Inorg. Chem.* **1981**, *20*, 3260−3267.

[8] L. Saussine, E. Brazi, A. Robine, H. Mimoun, J. Fischer, R. Weiss, *J. Am. Chem. Soc.* **1985**, *107*, 3534−3540.

[9] [9a] E. T. Farinas, C. V. Nguyen, P. K. Mascharak, *Inorg. Chim. Acta* **1997**, *263*, 17−21. [9b] F. A. Chavez, P. K. Mascharak, *Acc. Chem. Res.* **2000**, *33*, 539− 545.

[10] W. O. Siegl, *J. Heterocyclic Chem.* **1981**, *18*, 1613−1618.

[11] R. R. Gagné, R. S. Gall, G. C. Lisensky, R. E. Marsh, L. M. Speltz, *Inorg. Chem.* **1979**, *18*, 771−781.

[12] [12a] A. W. Addison, P. J. Burke, K. Henrick, *Inorg. Chem.* **1982**, *21*, 60−63. [12b] E. Balogh-Hergovich, J. Kaiser, G. Speier, G. Huttner, A. Jacobi, *Inorg. Chem.* **2000**, *39*, 4224−4229. [12c] O. P. Anderson, A. la Cour, A. Dodd, A. D. Garrett, M. Wicholas, *Inorg. Chem.* **2003**, *42*, 4513−4515.

[13] [13a] R. D. Bereman, G. D. Shields, J. R. Dorfman, J. Bordner, *J. Inorg. Biochem.* **1983**, *19*, 75−93. [13b] D. M. Baird, W. P. Maehlmann, R. D. Bereman, P. Singh, *J. Coord. Chem.* **1997**, *42*, 107−126.

[14] R. K. Hocking, T. W. Hambley, *Inorg. Chem.* **2003**, *22*, 2833−2835.

[15] [15a] F. Haber, R. Willstädter, *Chem. Ber.* **1931**, *64*, 2844−2856. [15b] F. Haber, J. Weiss, *Naturwiss.* **1932**, *51*, 948−950. [15c] F. Haber, J. Weiss, *Proc. R. Soc.* **1934**, *147*, 332−351.

[16] P. J. Domaille, R. L. Harlow, S. D. Ittel, W. G. Peet, *Inorg. Chem.* **1983**, *22*, 3944−3952.

[17] W. O. Siegl, F. C. Ferris, P. A. Mucci, *J. Org. Chem.* **1977**, *42*, 3442−3443.

[18] Nonius *OpenMoleN, Interactive Structure Solution*, Delft, **1997**.

[19] D. T. Cromer, J. T. Waber, *International Tables for X-ray Crystallography*, The Kynoch Press, Birmingham, **1974**.

Received January 8, 2004
Early View Article
Published Online May 5, 2004